ORIGINAL PAPER

The Effect of N-methylation on Photophysical Properties of 3-Aminoquinoline

Shipra Agarwal

Abstract It has been reported previously that the photophysics of 3-aminoquinoline (3AQ) is governed by a flip–flop motion of its amino group in apolar solvents and intersystem crossing in polar solvents. The nonradiative rates are governed by more than one solvent parameters, like polarity and hydrogen bonding ability of the solvent. So, 3AQ is not a well-behaved probe of any individual solvent parameter. In the present work, 3AQ has been modified synthetically; replacing an amino hydrogen atom with a methyl group and photophysical properties were studied in 22 different apolar, polar-aprotic and polar-protic solvents. It is found that Stokes' shifts and fluorescence quantum yields exceptionally low in apolar solvents as compared to those in other solvents. Such substitution causes a decrease in the extent of the effect of the hydrogen bonding ability of the solvent and that nonradiative rate become a more regular function of polarity. However, the flip–flop appears to continue to be the major nonradiative pathway, as the nonradiative rates decrease with increase in micropolarity.

Keywords Quinoline · Fluorescent probe · Time resolved fluorescence · Intramolecular charge transfer · Empirical micropolarity

S. Agarwal (✉)
Department of Chemistry,
Indian Institute of Technology Bombay,
Powai, Mumbai 400 076, India
e-mail: ashipra@chem.iitb.ac.in

Introduction

Aminoquinolines are a class of molecules with interesting fluorescence properties [1–3]. This has prompted our group to initiate a systematic investigation on 3-Aminoquinoline (3AQ). The functionalization of such molecules are easy due to the presence of amino group and can be used further as possibility of enhancement in substrate binding, which has great importance in sensing technology [4–6]. 3AQ in apolar solvents, exists in non-planar configurations, in which its -NH$_2$ group is very flexible and do not participate in resonance with quinoline moiety. The amino group undergo flip–flop motions and thereby couple to the solvent modes to efficiently deactivate the excited state in apolar solvents. While in polar and hydrogen bonding solvents photophysics of 3AQ is governed by intramolecular charge transfer (ICT). Thus, its fluorescence parameter are governed by an intricate interplay of polarity and hydrogen bonding ability [7, 8]. Such complications in its photophysics make 3AQ an ill-behaved fluorescent probe for microenvironments. However, the amino group in the compound renders it susceptible to synthetic modification and provides an opportunity of testing the hypothesis of the involvement of flip–flop motion and hence, the hydrogen bonding with solvent molecules. Such modification also opens up the possibility of the design of well-behaved fluorescent probes, by elimination of the factors that complicate the photophysics of 3AQ [7]. In the present work, hydrogen atom of amino group of 3AQ has been replaced with methyl group, as a result of this a new compound *viz.*, N-methylquinolin-3-amine (NMeAQ) has been synthesized for the first time and the effect of solvents on its photophysical properties have been investigated. In the synthetic procedure of monomethylaion, at first ionization of N-H bond take place and then alkylation occur

which requires an inert atmosphere because highly reactive N-anions are generated during the reaction (Scheme 1) [9]. The fluorescence properties of this newly synthesized molecule have been studied in 22 organic solvents (apolar, polar-aprotic and polar-protic) using ground-state absorption and steady-state and time-resolved fluorescence measurements, in order to understand the effect of N-methylation on the excited state processes. In NMeAQ, very large Stokes' shifts are observed which are very sensitive to the solvent polarities and micropolarities. Due to these interesting properties, such compound can have applications in studying the solvatochromic behaviours and polarities of different environments and also in measuring the solvent relaxation times using dynamic Stokes' shift method.

Experimental

Synthesis of N-methylquinolin-3-amine

To a 250-mL, three-necked, round-bottomed flask equipped with a magnetic stirring bar, an argon inlet, a 100-mL pressure-equalizing addition funnel, and a rubber septum, flushed with argon, 2.28 g (0.02 mol) of a 35% dispersion of potassium hydride (KH) in mineral oil was added. The mineral oil was removed by introducing 15 mL of hexane with a syringe and stirred gently, followed by removal with a syringe after potassium hydride settled down. To this flask 75 mL of dry tetrahydrofuran (THF) was added, followed by gradual addition of a solution of 1.44 g (0.01 mol) of 3-aminoquinoline in 23 mL of dry THF, using a dropping funnel. The magnetically stirred suspension of potassium hydride is cooled to 0 °C, and the solution of 3-aminoquinoline was added dropwise over a 10-min period. After complete addition, the mixture was stirred at 0 °C for 20 min, and 3.4 mL (0.052 mol) of methyl iodide was introduced dropwise via syringe. The cooling bath was removed, and the reaction mixture was stirred at room temperature for 10 hr. The reaction was quenched by cautious addition of 5 mL of water, and the resulting mixture was transferred to a 500-mL separatory funnel containing 35 mL of water. The layers were separated, and the aqueous layer was extracted three times with 30 mL of ethyl acetate. The combined organic extracts were washed with 75 mL of saturated sodium chloride solution, dried

over magnesium sulfate, and concentrated by rotary evaporation to give crude product. Crude product was dissolved in 5 mL ethylacetate and decolorized with Norit SA3 (100 mesh) activated charcoal reflux. The solution was cooled to room temperature and filtered through celite pad using vacuum filtration. Finally filtrate was concentrated using rotary evaporator and at low temperature (8–10 °C) needle like crystals appeared after 1 day. N-methylquinolin-3-amine is obtained in 32% yield (0.49 g). R_f, 0.8, (DCM: MeOH::8:2, v/v), UV (MeOH): λ_{max} 368 nm; ^1H NMR (CD$_3$OD, 400 MHz, δ (ppm)): 2.78 (s, 3H); 4.88 (s, -NH); 7.4 (t, 1H, J=6.4); 7.45–7.6 (m, 2H); 7.78–7.92 (m, 2H); 8.02 (d, 1H, J=8.2); ^{13}C NMR (CD$_3$OD, 100 MHz, δ (ppm)): 29.6 (NHCH$_3$), 124.8 (6-C), 125.1 (8-C), 126.1 (7-C), 127.3 (8-C), 129.1 (4-C), 129.7 (5-C), 137.5 (3-C), 141.5 (10-C), 143.5 (2-C); MS (EI) m/z: 158.08 (M+); Anal. Cacld for C$_{10}$H$_{10}$N$_2$ C, 75.92; H, 6.37; N, 17.71; found: C, 75.91; H, 6.39; N, 17.68 (Figure S1 a, b, c in supporting information).

Photophysical Studies

3-Aminoquinoline from Lancaster, UK is used as received to synthesize the N-methylquinolin-3-amine (NMeAQ). The purity of NMeAQ was confirmed from the comparative study of its fluorescence excitation spectra and absorption spectra given in supporting information (Figure S2) which shows that excitation and absorption spectra corresponds and there is only one species, which doesn't has any form (aggregates, complexes etc) in ground state. Millipore water is used for spectroscopic studies. Other solvents of spectroscopic grade from Spectrochem, Mumbai, India are distilled immediately prior to use. The steady state spectra were recorded on JASCO V570 spectrophotometer and Varian Cary Eclipse fluorimeter. Fluorescence quantum yields (ϕ_f) of NMeAQ in different organic solvents are calculated after proper correction for changes in absorbance using quinine sulphate dissolved in 0.5 M H$_2$SO$_4$ as the standard, (ϕ_f=0.55) [10]. For all the fluorescence measurements, the optical density (OD) of the solutions have kept quite low (<0.2) at the excitation wavelength. Time-resolved fluorescence measurements are performed with TCSPC fluorescence spectrometer with R3809U-50 microchannel plate photomultiplier tube (MCP-PMT, Hamamatsu) and Picoharp300 TCSPC module using an IBH light emitting diode with λ_{ex}=341 nm and repetition rate of 1 MHz as the source. The full width at half
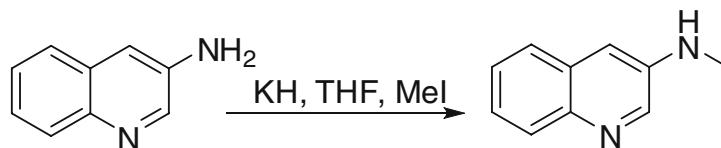
Scheme 1 Synthesis of methylated derivative (NMeAQ) of 3-aminoquinoline

maximum of the instrument response function is 800 ps. The emission from the samples is collected at right angle to the direction of the excitation beam, at magic angle polarization (54.7°), except for the anisotropy measurements. The data are fitted to single function after deconvolution of the instrument response function by an iterative reconvolution technique, using the IBH DAS 6.2 data analysis software, where reduced χ^2 and weighted residuals serve as parameters for goodness of fit [11]. Non-radiative rate constants in different solvent have been calculated from steady state fluorescence quantum yield (ϕ_f) and radiative lifetimes (τ_f) using the relation $k_{NR} = (1 - \phi_f)/\tau_f$.

In order to find out the solvent polarity effect on NMeAQ, Lippert- Mataga equation has been used,

$$\Delta\upsilon = \frac{2\Delta\mu^2}{hca^3}\left(\frac{\varepsilon - 1}{2\varepsilon + 1} - \frac{n^2 - 1}{2n^2 + 1}\right) + constant \quad (1)$$

$$\Delta f = \left(\frac{\varepsilon - 1}{2\varepsilon + 1} - \frac{n^2 - 1}{2n^2 + 1}\right) \quad (2)$$

where $\Delta\upsilon$ is frequency shift (in cm^{-1}) between absorption and emission, and Δf is polarity function. ε and n are dielectric constants, refractive index, respectively, of the solvents. Their values have been obtained from literature [12–14]. Kamlet-Taft (KT) analysis has been performed on the absorption and fluorescence maxima in different solvents, so as to ascertain the relative contributions of solvent polarity and hydrogen bonding effect on the spectra of the fluorophore. In this analysis, the spectral maxima are fitted to a weighted linear sum of the polarity and hydrogen bonding abilities of the solvent [15, 16].

$$\upsilon = \upsilon_0 + p\pi^* + a\alpha + b\beta \quad (3)$$

where υ denotes the spectral peak frequency in a particular solvents, π^* denotes the dipolarity-polarizability, α and β denote the hydrogen-bond donating (HBD) and hydrogen-bond accepting (HBA) ability of the solvent and ν_0 denotes the peak frequency in absence of any solvent. The value of the coefficient p, a, b (obtained from analyzing the spectral parameters in a series of solvents) gives an idea about the effect of polarity and HB on the spectral properties of a fluorophore.

Results and Discussion

Photophysical Properties

Solvent Dependence on Steady State Absorption and Fluorescence Spectra

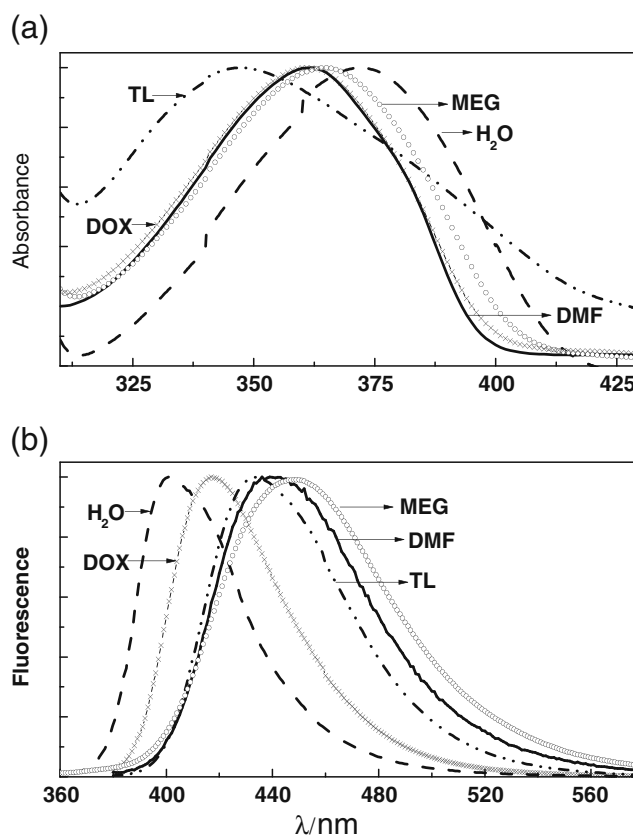UV/Vis absorption and fluorescence spectra of NMeAQ in apolar and polar solvents are depicted in Fig. 1. The

Fig. 1 **a** Absorption spectra and **b** Emission spectra of NMeAQ in different solvents: toluene (TL), dioxane (DOX), dimethylformamide (DMF), ethanediol (MEG) and water (H$_2$O)

photophysical properties strongly change with respect to 3-AQ as can be seen in Table 1. Table 1 lists photophysical characteristics of NMeAQ in different organic solvents. The maxima of absorption and emission spectra are red shifted with increase in the polarity of the solvents in NMeAQ compared to that in 3AQ. This is reminiscent of the situation in 7-amino coumarin, in which N-methylation causes a red shifted absorption and emission spectra [17, 18]. But water shows anomalous behaviour, absorption spectra in water is remarkably blue shifted while emission spectra is red shifted. This is due to increase in charge transfer character in excited state.

Typical stokes shift values are 2,475 cm-1 in n-hexane (apolar), 4,162 cm-1 in acetonitrile (polar aprotic) and 3,918 cm-1 in methanol (polar protic) in NMeAQ. The corresponding Stokes shifts are 2,735, 3,456 and 3,941 cm-1 in 3AQ. Thus, the Stokes shifts are greater in NMeAQ than in 3AQ in polar solvents. However this value is less in NMeAQ in apolar solvent. In apolar solvents the emission spectra are distinctly blue shifted than that observed in polar solvents. This indicates that NMeAQ is more destabilized in excited state than ground state in apolar solvent. The appearance of the $\overline{\upsilon}_{abs}$ and $\overline{\upsilon}_{ems}$ (Fig. 2(a)) at higher energies in these solvents indicates an interesting

Table 1 Spectral and temporal parameters for NMeAQ in organic solvents

	Solvent	Δf	λ_{abs}^{max} (nm)	λ_{ems}^{max} (nm)	$\Delta\upsilon$ (cm^{-1})	ϕ_f	τ_f (ns)	$k_{NR} \times 10^9$(S^{-1})	$k_R \times 10^9$(S^{-1})
Non-polar solvents	n-Hexane	0	354	388	2,475	0.057	1.06	0.89	0.05
	n-Hexane [a]	0	336	370	2,735	0.16	1.19	0.70	0.13
	n-Heptane	0	355	387	2,329	0.053	1.08	0.87	0.049
	Cyclohexane	0	355	388	2,395	0.056	1.19	0.80	0.047
	3-Methylpentane	0	354	389	2,541	0.050	1.06	0.83	0.047
	Toluene	0.013	362	401	2,686	0.12	2.2	0.31	0.054
Polar-aprotic solvents	1,4-Dioxane	0.025	361	417	3,720	0.31	5.54	0.15	0.056
	Ethylacetate	0.201	365	419	3,530	0.14	3.2	0.24	0.044
	THF	0.212	360	418	3,854	0.24	3.21	0.19	0.074
	DMSO	0.264	372	436	3,945	0.68	9.31	0.04	0.073
	DMF	0.273	365	428	4,032	0.60	7.76	0.11	0.077
	Acetone	0.284	362	423	3,983	0.33	4.7	0.15	0.070
	Acetonitrile	0.305	364	429	4,162	0.45	6.31	0.14	0.071
	Acetonitrile[a]	0.305	346	393	3,456	0.31	2.01	0.34	0.15
Polar-protic solvents	1-Hexanol	0.244	367	426	3,773	0.39	8.41	0.07	0.046
	1-Pentanol	0.249	368	425	3,644	0.37	8.05	0.08	0.046
	t-Butanol	0.262	364	426	3,998	0.35	5.94	0.11	0.059
	1-Butanol	0.263	367	427	3,828	0.34	7.99	0.04	0.042
	1-Propanol	0.274	367	426	3,773	0.18	7.98	0.11	0.022
	iso-Propanol	0.276	366	425	3,792	0.13	7.62	0.11	0.017
	Ethanediol	0.279	372	436	3,945	0.11	2.56	0.26	0.0427
	Ethanol	0.288	367	428	3,883	0.28	7.96	0.06	0.035
	Methanol	0.308	368	430	3,918	0.12	2.71	0.33	0.044
	Methanol[a]	0.309	350	406	3,941	0.68	4.76	0.06	0.14
	Water	0.319	347	448	6,497	0.09	2.38	0.38	0.037

[a] data shown is for 3AQ (in hexane, acetonitrile and methanol) and taken from reference no [7].

The spectral and temporal parameters in Table 1 are polarity function (Δf), absorption maxima (λ_{abs}^{max}), emission maxima (λ_{ems}^{max}) Stokes shift ($\Delta\upsilon$), Fluorescence quantum yields (ϕ_f), radiative lifetimes (τ_f), nonradiative rate constants (k_{NR}), radiative rate constants (k_R). Abbreviations for the solvents are tetrahydrofuran (THF), dimethyl sulfoxide (DMSO) and dimethyl formamide (DMF).

observation that no specific solute–solvent interaction is expected in apolar solvents, for which I have tried to correlate the Stokes' shifts (i.e., $\Delta\overline{\upsilon} = \overline{\upsilon}_{abs} - \overline{\upsilon}_{ems}$) with the Δf *values* of the solvents. It is generally implicit that the longer-wavelength absorption and the fluorescence bands of a molecule are due to the transitions between the same two ground and excited electronic states [19–22] and thus, the Stokes' shifts can be correlated with the solvent polarities of different solvents. Higher $\overline{\upsilon}_{abs}$ and $\overline{\upsilon}_{ems}$ values in aprotic solvents than those in other protic solvents of similar polarities indicate that the S$_0$ and S$_1$ states of NMeAQ are not of the same nature. Figure 2(b) shows the Lippert plot, which is almost liner with some deviations for almost all the solvents except apolar solvents which have unusually small Stokes' shift. Another interesting point to be noted from Fig. 2(b) is in relation to the highly viscous alcoholic solvent; t-Butanol (^{t}BuOH) has linear correlation with DMSO and DMF solvents and has upward deviation than other protic solvents. This indicates intermolecular

hydrogen bonding interaction between NMeAQ and the solvent molecules, which causes an extra stabilization for both S$_0$ and S$_1$ states of the compound. All other protic solvents are in linear and a little lower in to the corelation observed for aprotic solvents.

Involvement of the planar or the nonplanar structure both are expected in the ground state of the compound, depending on the solvent polarities. It is expected that in apolar solvents, nonplanar structure will have energies lower than those of the planar structure even in the ground state. Thus, in apolar solvents, since both ground and excited states of NMeAQ are apolar with no resonance between the NHMe group and the quinoline moiety, the $\overline{\upsilon}_{abs}$ and $\overline{\upsilon}_{ems}$ appear at much higher energies compared to those in other solvents of moderate to higher polarities. For the same reason, the $\Delta\overline{\upsilon}$ values in apolar solvents are expected to be much smaller compared to those in other solvents. Since both the ground and excited states of NMeAQ are of ICT character in moderate to higher polarity
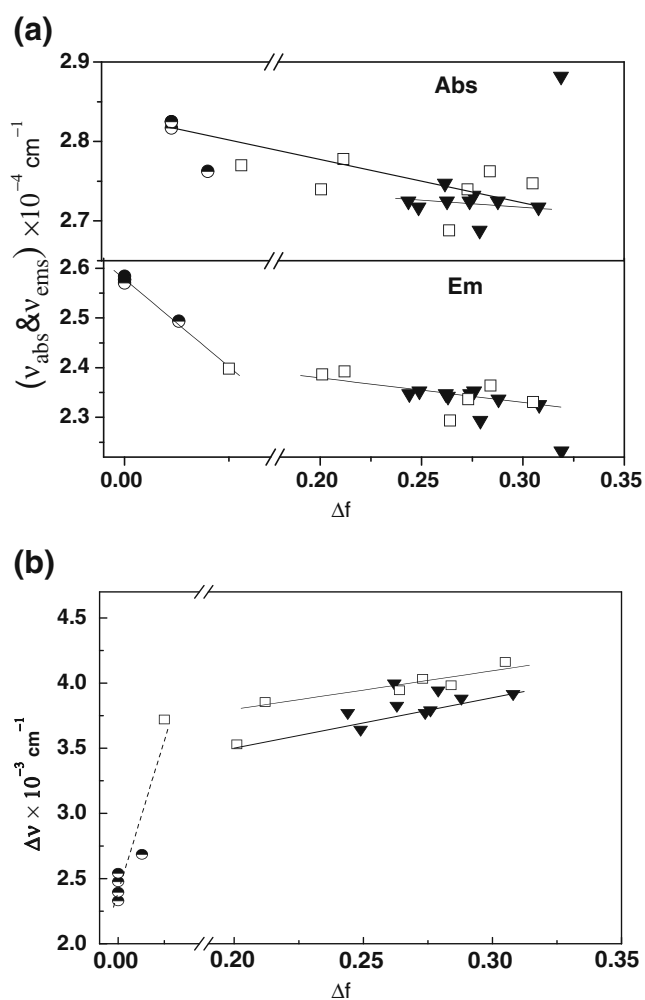
(a)

(b)

Fig. 3 The fluorescence decay profiles of NMeAQ in *n*-hexane, 1,4-dioxane, acetonitrile and methanol

Fig. 2 a Plot of energies of absorption ($\bar{\nu}_{abs}$) and emission ($\bar{\nu}_{em}$) against solvent polarity function (Δf). **b** Plot of Stokes shift ($\Delta\bar{\nu}$) against solvent polarity function (Δf) in apolar (*solid triangle*), aprotic (*hollow circle*), and protic (*solid circle*) solvents. The reported data are in the following solvent systems in the order of increasing polarity: (*1*) *n*-heptane, (*2*) *n*-hexane, (*3*) cyclohexane, (*4*) 3MP, (*5*) toluene (*6*) 1,4-dioxane, (*7*) ethyl acetate, (*8*) tetra hydrofuran, (*9*) dimethyl formamide, (*10*) DMSO, (*11*) acetone, (*12*) acetonitrile, (*13*) 1-hexanol, (*14*) 1-pentanol, (*15*) ᵗBuOH, (*16*) 1-BuOH, (*17*)1-propanol, (*18*) iso-propanol, (*19*) ethanol, (*20*) ethanediol (*21*) methanol (*22*) water. (*For abbreviations see* Table 1)

solvents, the $\bar{\nu}_{abs}$ and $\bar{\nu}_{ems}$ undergo substantial red shift with solvent polarity.

The fluorescence quantum yields, in the plot of ϕ_f versus the $E_T(30)$ (Figure S3(b) in supporting information) and ϕ_f versus the Δf, first increase with increasing Δf and $E_T(30)$ and then after DMSO it decreases for higher Δf and $E_T(30)$ values with significant downward deviation in protic solvents. This is usual; as generally, an increased Stokes' shift is accompanied by a decrease in fluorescence quantum yield due to an increase in nonradiative rates, as per the energy gap law [23]. Figure 3 shows the radiative lifetimes in four different solvents. Notably, the fluorescence decays
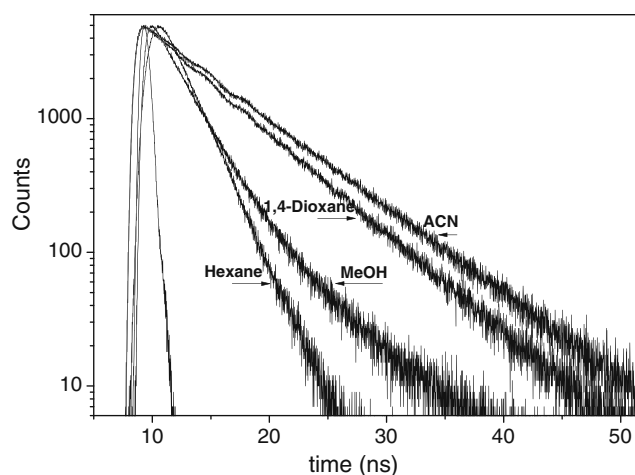
are single exponential in all apolar solvents and polar solvents except water and ethanediol. This is reminiscent of the situation in aminoquinoline and aminocoumarins, where the tetrahedral amino group is considered to undergo flip–flop motion in apolar solvents, thereby providing an additional nonradiative pathway for depopulation of the excited state in these solvents [24, 25]. The flip–flop motion is proposed to be restricted in polar solvents due to formation of the planar ICT state. The greater suppression of the nonradiative process in protic solvents and DMSO is rationalized by specific hydrogen bonding interactions. The presence of one hydrogen atom in amino group in NMeAQ leads us to offer a similar explanation for the observations that has been obtained in 3AQ.

Fluorescence quantum yields (ϕ_f) of NMeAQ in different solvents were estimated at room temperature and are listed in Table 1. It is clear from the plot of ϕ_f versus the Δf values (Fig. 4(b)) that ϕ_f values in apolar solvents are lower in comparison to other solvents and it increases with increasing Δf and it is maximum for DMSO i.e. a weak, but distinct, linear variation can be obtained in solvents of low to medium polarity as well and for these solvents, the line has a positive slope while in case of polar protic solvents there is also a linear variation with negative slope for increasing polarity, this reduction in the ϕ_f values attribute to the intermolecular hydrogen bonding effect. From the above data it was inferred that solvent polarity effect on spectral shifts that the S_0 and S_1 states of NMeAQ in apolar solvents are of different characteristics than in other solvents because of this ϕ_f values in apolar solvents are quite different than those in other solvents.

In order to explore this possibility further, the dependence of the radiative and nonradiative rates as a function of solvent polarity has been examined. In this study, the empirical micropolarity parameter, $E_T(30)$ has also been
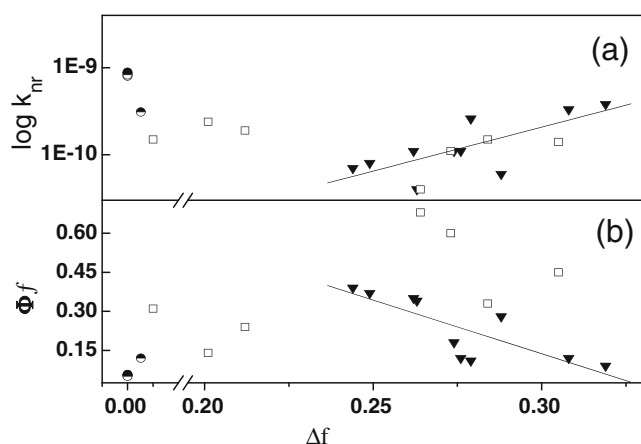
Fig. 4 A linear variation of the non-radiative rate (**a**) and quantum yield (**b**) with the solvent polarity function (Δf). The data in apolar (*circle*), aprotic (*hollow square*), and protic (*solid triangle*), The solid line is linear fit

used with Δf, as some kind of a specific solute–solvent interaction at the molecular level is suspected to operate and in such cases, it is well established that $E_T(30)$ is a more useful polarity parameter compared to measures of bulk polarity like the dielectric constant [26]. The values of radiative rate constants (k_R) are found to be almost constant for all the solvents used, but the non-radiative rate constants (k_{NR}) exhibit a rather interesting solvent dependence (Table 1). While observing the plot of log k_{NR} rates with the empirical solvent polarity parameter $E_T(30)$ (Figure S3 (a)) it yields a straight line with a positive slope for the high-polarity solvents and for low polarity the log k_{NR} values decreases linearly with increasing micropolarity from apolar to polar aprotic solvents i.e. it yields straight line with negative slope with some deviations. The log k_{NR} in DMSO turns out to be smaller than other solvents of similar polarity. Thus, the polarity dependence appears to generally decrease with increasing polarity, with the breaks in the trends signifying the onset of a different kind of mechanism that influences the nonradiative process. Similar to the case of aminocoumarins, the tetrahedral amino group in 3AQ can undergo flip–flop motion in apolar solvents. The apolar excited state with tetrahedral amino group is destabilized with increase in the polarity of the solvent, in comparison to

the more polar ICT state which is planar. The sudden decrease of the k_{NR} between $E_T(30)$ 31.1 and 35 can be rationalized as a crossover from the predominantly apolar pyramidal conformation of the amino group to the predominantly planar one. The sudden increase, on crossing over to protic solvents, can be explained by further less hindered motion of the amino group as compared to 3AQ due to the formation of hydrogen bonds. A similar explanation can be offered for the even greater decrease in the nonradiative rate in DMSO and tBuOH. The protic solvents act as hydrogen bond donors as well as acceptors. DMSO, on the other hand, acts only as a hydrogen bond acceptor. The lone pair on the nitrogen atom involves in hydrogen bonding with the protic solvent molecules and reduces its participation in the ICT process, this interaction is absent in DMSO. Thus, in this solvent, the movement of the amino group is restricted by the hydrogen bonds between amino nitrogen atoms and the solvent molecule, but the lone pair is absolutely free to participate in ICT, thereby restricting the motion of the amino group to an even greater extent.

Nevertheless, it is important to note that two distinct regions with different types of dependence between non-radiative rates and polarity are identified. The considerable deviation of the data points on either side of the lines is too large to be entirely due to errors in the experiment. It is more likely that they indicate different kinds of specific solvent effects. For example, there is a negative deviation for highly viscous solvent ethylene glycol and positive deviation for acetone which contains C=O bond. Moreover, the question that arises now is that whether the so-called unusual behavior is observed in the low-polarity or the high polarity region, as there are weak linear correlations of opposite natures in the two regions. At this point, it is useful to recall that in the absence of excited state reactions like twisted intramolecular charge transfer (TICT), excited state proton transfer (ESPT), photoisomerization etc., *log* k_{NR} can have a direct as well as inverse variation with solvent polarity, depending on the relative polarities of the ground and the excited states. In molecules with a more polar excited state than the ground state, there is a Stokes shifted emission quantified by the well-known Lippert

Table 2 KT analysis of absorption and emission peak frequencies and ln k_{NR} for NMeAQ

		p(π^*)	a(α)	b(β)	ν_0	R
NMeAQ	Abs	−617 (55%)	−494 (43%)	−28 (2%)	28,039	0.97
	Em	−2,066 (68%)	−481 (16%)	−456(16%)	25,308	0.92
3AQ[a]	Abs	−975 (55%)	−681 (39%)	−100 (6%)	29,736	0.97
	Em	−1,559 (47%)	−1,088 (33%)	−659 (20%)	26,948	0.98

[a] Data taken from reference no. 7. For absorption and emission, units are in cm^{-1}. The figures in parentheses indicate the relative percentage. R denotes regression coefficient.

Table 3 Relevant geometrical parameters involved in photophysical properties of NMeAQ

	B3LYP/gas	Onsager/H$_2$O	CIS
C2-N2-H	115.19	115.62	115.46
C2-N2-Me	121.87	121.84	125.07
H1-N2-Me	115.89	115.76	116.03
C1-C2-N2-H	−19.86(−25.0)	−19.04(−34.4)	−6.42(−13.0)
C3-C2-N2-Me	12.38(22.5)	12.72(17.9)	17.70(21.8)

Ground State (B3LYP, Onsagar) and excited state (CIS) calculations are performed using 6-311++G** and 6-31+G* respectively. Paranthesis contains corresponding value for 3AQ ref. no 7.

Mataga equation [27]. Moreover, in this kind of molecules as the energy gap between the excited and the ground state decreases in polar solvents, there is an increase in the non-radiative rate with polarity [28, 29]. The increase in the energy gap between their ground and excited states forms the basis of the widely used E$_T$(30) scale of polarity as observed in Lucifer yellow ethylenediamine (LYen).

Kamlet-Taft Analysis of the Spectral Data

Micropolarity is not only the parameter which effect on photophysical behavior of fluorophore. Other parameters like hydrogen bonding donation ability (α) and hydrogen bonding accepting ability (β) may also play important roles when the fluorophore has both acid and basic group. In such a situation it is convenient to approach a linear solvation energy relationship proposed by Kamlet and Taft [30–33]. Such a treatment has been performed earlier on 3AQ [7]. Upon performing a similar multiple regression fitting of the data of NMeAQ in all solvents to Kamlet Taft (KT) function, the following are observed: The relative contributions of polarity and hydrogen bonding ability, towards the absorption maxima of NMeAQ and 3AQ are the same. This indicates that the ground state intramolecular interaction in NMeAQ is more or less the same as in 3AQ. The relative contribution of polarity to emission, however, is increased to 68% in NMeAQ, as against 47% in 3AQ (Table 2). Moreover, equal contributions are observed from α and β, unlike in 3AQ where the contribution from β was

more than that from α. Thus the fluorescence of the NMeAQ is found to be influenced more by the polarity and less by the hydrogen bonding ability of the medium, than that of 3AQ. This observation is commensurate with the inference drawn in the previous section.

Density Functional Theory Calculations

Geometrical Features and Natural Bond Orbital Analysis

The geometry of the neutral form of NMeAQ has been optimized independently using the Density functional theory (DFT) (Table 3). The co-planarity of the methyl substitute amino group with ring system play an important role in the possibility of flip–flop motion of the methyl substituted amino group and intramolecular charge transfer (ICT) in the system. Hence the bond angle C2-N2-H, C2-N2-Me, Me-C-H and the H/Me-N2-C-C dihedral angles (dh) obtained from different level of calculation shown in Table 3 provide an idea about the feasibility of the flip-flop motion. It is seen that the value dihedral angle (dh) 'C1-C2-N2-H' decreases in excited state from −19.86° (dh in ground state) to −6.42° where as value of the dihedral angle 'C3-C2-N2-Me' increases in the excited state in NMeAQ. However comparing the corresponding dihedral angles shown in parentheses in Table 3 for 3AQ, it is clear that the degree of planarity of the methyl substituted amino group in NMeAQ in excited state is less than that of amino group in 3AQ. This indicates some hindrance in flip-flop motion of the substituted methyl group which slows down the non-radiative process in apolar and polar aprotic solvent. The theoretical calculation also supports the occurrence of the ICT state though the planarity in the excited state is less in compare to that in 3AQ. Experimentally it has been observed that the red shifted absorption and emission almost in all solvents. This is due to increase in charge transfer character in excited state. This can be interpreted via, natural bond orbital (NBO) analysis [34] which has been performed at B3LYP/6-311++G** level of theory and the respective results is presented in Table 4. The perturbation E(2) charge-transfer energies corresponding to the interaction of lone pair of N2 with antibonding (π*)

Table 4 Second order perturbation theory analysis of Fock matrix in NBO basis for NMeAQ

Donor (i)	Acceptor (j)	[a]E(2)/kcalmol^{-1}	[b]E(j)-E(i)/a.u.	[c]F(i,j)/a.u.
[d]LP N$_1$	σ* (C$_4$–C$_5$)	9.36	0.88	0.082
LP N$_1$	σ* (C$_1$–C$_2$)	10.36	0.84	0.084
LP N$_2$	π* (C$_2$–C$_3$)	36.95	0.30	0.097

$E(2) = -n_\sigma \frac{\langle \sigma | F | \sigma \rangle}{\varepsilon_{\sigma^*} - \varepsilon_\sigma} = -n_\sigma \frac{F_{ij}^2}{\Delta E}$; [a] E(2) means energy of hypercongugative interactions, [b] energy difference between donor and acceptor i and j NBO orbitals, [c] F(i,j) is the Fock matrix element between i and j NBO orbitals, n$_\sigma$ is the population of the donor σ orbital. [d] LP=lone pair.

orbital of C_2-C_3 is 8 kcal/mole more in NMeAQ than in 3AQ [7]. This clearly indicates an increase in charge transfer character with substitution of methyl group. The other parameters which are obtained in NBO analysis are energy difference ($\Delta E_{i,j}$) in between donor and acceptor orbital which is 0.30 a.u. and Fock matrix element($F_{i,j}$) which is 0.097.

From the solvent polarity effect on the Stokes' shifts in moderate to higher polarity solvents, it is clearly indicated that the S_1 state of NMeAQ is of ICT character. From the structural point of view, the ICT state is expected to have a planar configuration with the N-quinoline ring bond. In this configuration, since the amino group is quite rigidly bound to the quinoline moiety, there is hardly any flexibility for this group. Thus, in the ICT structure, it is expected that the nonradiative deactivation process will be quite slow, resulting in high Φ_f and τ_f values for the dye. In apolar solvents, since no specific solute–solvent interaction is expected, the unusual blue shift in the $\bar{\nu}_{abs}$ and $\bar{\nu}_{ems}$ values (Fig. 2a) and the exceptionally lower $\Delta\bar{\nu}$ values (Fig. 2b) indicate that the S_1 state of NMeAQ must exist in a apolar structure in these solvents. It is thus logical to think that in apolar solvents the 3-NHMe group of NMeAQ might remain as a free substituent without participating in resonance with the quinoline moiety.

Conclusions

Above evidences shows, NMeAQ emerges as a more 'well-behaved' fluorescent probe than 3AQ. A good correlation with bulk polarity and micropolarity is also observed, though. Experimental and computational results indicate the occurrence of excited state intramolecular charge transfer to a greater extent than in 3AQ. However, the flip–flop motion of the substituted amino group remains the predominant nonradiative process, as the nonradiative rate decreases with increase in the polarity of the medium but in protic solvents, the ICT state has a major contribution to the photophysics of the fluorophore. The "well-behaved" nature arises from a decrease in the hydrogen bonding ability of the methyl-substituted molecule, which obliterates the complications observed earlier in the excited state dynamics of 3AQ, which had arisen out of an intricate interplay of polarity and hydrogen bonding ability. This observation is a justification, albeit indirect, of our earlier explanation of the intriguing photophysics of 3AQ.

References

1. Egan TJ, Kaschula HC, Marques MH, Misplon A, Walden J (2000) Structure-function relationships in aminoquinolines: effect of amino and chloro groups on quinoline-hematin complex formation, inhibition of â-hematin formation, and antiplasmodial activity. J Med Chem 43:283–291
2. Kaschula HC, Egan TJ, Hunter R, Basilico N, Parapini S, Taramelli D, Pasini E, Monti D (2002) Structure−activity relationships in 4-aminoquinoline antiplasmodials: the role of the group at the 7-position. J Med Chem 45:3531–3539
3. Farruggia G, Iotti S, Prodi L, Montalti M, Zaccheroni N, Savage PB, Trapani V, Sale P, Wolf FI (2006) 8-Hydroxyquinoline derivatives as fluorescent sensors for magnesium in living cells. J Am Chem Soc 128:344–350
4. Xu G, Tarr AM (2004) A novel fluoride sensor based on fluorescence enhancement. Chem Comm 1050
5. Otón F, Tárraga A, Velasco DM, Espinosa A, Molina P (2004) A new fluoride selective electrochemical and fluorescent chemosensor based on a ferrocene–naphthalene dyad. Chem Comm 1658
6. Kato R, Cui Y-Y, Nishizawa S, Yokobori T, Teramae N (2004) Thiourea–isothiouronium conjugate for strong and selective binding of very hydrophilic $H_2PO_4^-$ anion at the 1,2-dichloroethane–water interface. Tetrahedron Lett 45:4273
7. Panda D, Datta A (2006) The role of the ring nitrogen and the amino group in the solvent dependence of the excited-state dynamics of 3-aminoquinoline. J Chem Phys 125:54513
8. Schulman SG, Capomacchia AC (1972) Excited state prototropism and solvent dependence of 3-amino quinoline. Anal Chim Acta 58:91–99
9. Sorokin VI, Ozeryanskii VA, Pozharskii AF (2003) A simple and effective procedure for the n-permethylation of amino-substituted naphthalenes. Eur J Org Chem 496
10. Eaton DF (1988) Reference materials for fluorescence measurement. Pure Appl Chem 60:1107–1114
11. Burai TN, Panda D, Datta A (2008) Fluorescence enhancement of epicocconone in its complexes with cyclodextrins. Chem Phys Lett 455:42–46
12. Dean JA (1987) Lange's handbook of chemistry, 163rd edn. McGraw-Hill, New York
13. Mataga N, Kaifu Y, Koizumi M (1956) Solvent effects upon fluorescence spectra and the dipole moments of excited molecules. Bull Chem Soc Jpn 29:465–470
14. Amthor S, Lambert C, Duemmler S, Fischer I, Schelter J (2006) Excited mixed-valence states of symmetrical donor-acceptor-donor π systems. J Phys Chem A 110:5204–5214
15. Kamlet MJ, Abboud JL, Abraham MH, Taft RW (1983) Linear solvation energy relationships. 23. A comprehensive collection of the solvatochromic parameters, π*, α, and β, and some methods for simplifying the generalized solvatochromic equation. J Org Chem 48:2877–2887
16. Marcus Y, Kamlet MJ, Taft RW (1988) Linear solvation energy relationships. Standard molar gibbs free energies and enthalpies of transfer of ions from water into nonaqueous solvents. J Phys Chem 92:3613–3622
17. Rechthaler K, Kühler G (1994) Excited state properties and deactivation pathways of 7-aminocoumarins. Chem Phys 99:189
18. Soujanya T, Fessenden RW, Samanta A (1996) The nature of 4-aminophthalimide-cyclodextrin inclusion complexes. J Phys Chem 100:3507
19. Birks JB (1970) Photophysics of aromatic molecules. Wiley-Interscience, New York

20. Becker RS (1969) Theory and interpretation of fluorescence and phosphorescence. Wiley-Interscience, New York
21. Lakowicz JR (1983) Principles of fluorescence spectroscopy, 3rd edn. Plenum Press, New York
22. Rohatgi-Mukherjee KK (1978) Fundamentals of photochemistry. Wiley Eastern, New Delhi
23. Turro NJ (1978) Modern molecular photochemistry. Benjamin, London
24. Nad S, Pal H (2001) Unusual photophysical properties of coumarin-151. J Phys Chem A 105:1097
25. Pal H, Nad S, Kumbhakar M (2003) Photophysical properties of coumarin-120: unusual behavior in apolar solvents. J Chem Phys 119:443
26. Panda D, Mishra PP, Khatua S, Koner AL, Suno RB, Datta A (2006) Anomalous excited-state dynamics of Lucifer yellow CH in solvents of high polarity: evidence for an intramolecular proton transfer. J Phys Chem A 110:5585
27. Seliskar CJ, Brand L (1971) Electronic spectra of 2-aminonaphthalene-6-sulfonate and related molecules. II. Effects of solvent medium on the absorption and fluorescence spectra. J Am Chem Soc 93:5414–5420
28. Rettig W, Majenz W, Herter R, Létard J-F, Lapouyade R (1993) Photophysics of stilbenoid dye systems: a comparison of experiment and theory. Pure Appl Chem 65:1699
29. Eisenthal KB (1996) Liquid interfaces probed by second-harmonic and sum-frequency spectroscopy. Chem Rev 96:1343–1360
30. Kamlet MJ, Abboud JL, Taft RW (1977) The Solvatochromic comparison Method 6. The π^* scale of solvent polarities. J Am Chem Soc 99(18):6027–6038
31. Kamlet MJ, Hall TN, Boykin J, Taft RW (1979) Linear solvation energy relationships. 6. Additions to and correlations with the π^* scale of solvent polarities. J Org Chem 44:2599–2604
32. Das K, Jain B, Patel HS (2006) Hydrogen bonding properties of coumarin 151, 500, and 35: the effect of substitution at the 7-amino position. J Phys Chem A 110:1698–1704
33. Molotsky T, Huppert D (2003) Site specific solvation statics and dynamics of coumarin dyes in hexane-methanol mixture. J Phys Chem A 107:2769–2780
34. Reed AE, Curtiss LA, Weinhold F (1988) Intermolecular interactions from a natural bond orbital, donor-acceptor viewpoint. Chem Rev 88:899–926